Available online at www.sciencedirect.com

ScienceDirect

Energy Procedia 63 (2014) 1296 – 1307

Energy Procedia

GHGT-12

Dynamic Modeling, Validation, and Time Scale Decomposition of an Advanced Post-Combustion Amine Scrubbing Process

Matthew S. Walters[a], Thomas F. Edgar,[a,b], Gary T. Rochelle[a]*

[a]McKetta Department of Chemical Engineering, The University of Texas at Austin, 200 E Dean Keaton St. Stop C0400, Austin 78712-1589, USA
[b]Energy Institute, The University of Texas at Austin, 2304 Whitis Ave. Stop C2400, Austin 78712-1718, USA

Abstract

Post-combustion amine scrubbing is a highly integrated process that uses extensive material and energy recycling to reduce costs and increase efficiency. As a result, the process variables exhibit a fast time scale at the unit level associated with the large recycle flows and a slow time scale at the plant level associated with the small feed and product flows. A reduced order model was developed for the system, and the material balances were demonstrated to be in nonstandard singularly perturbed form. Only the stripper vapor mole fractions evolve exclusively on the slow time scale in this model form; all other model states have both slow and fast components. By applying a variable transformation, the model is arranged into standard singularly perturbed form. The slow states in this form are the overall process material hold-ups as well as the stripper vapor mole fractions. An effective control strategy for the process should control the CO_2 removal rate and overall system inventory on the slow time scale using the small stripper overhead flowrate and a cascaded level setpoint controller, respectively. We show that attempting to control CO_2 removal rate with the large solvent recycle rate will likely lead to an ill-conditioned controller.

Peer-review under responsibility of the Organizing Committee of GHGT-12

Keywords: Singular Perturbation; Reduced Order Modeling; Time Scale Multiplicity

1. Introduction

The general trend in the chemical industry is the development of increasingly integrated process designs that use extensive material and energy recycling as well as minimize the overall chemical inventory. With large capital and operating costs, post-combustion amine scrubbing adheres to this trend. After the amine solvent has absorbed CO_2

* Corresponding author. Tel.: +1-512-471-7230; fax: +1-512-471-7060.
E-mail address: gtr@che.utexas.edu

Peer-review under responsibility of the Organizing Committee of GHGT-12
doi:10.1016/j.egypro.2014.11.138

from the flue gas, it is regenerated at high temperature and completely recycled back to the absorber. Most of the sensible heat from the thermal swing process is recovered either through direct contact packing or a cross heat exchanger. Designing an effective plantwide control strategy of processes with recycle streams is often complicated and is much less studied than systems without recycle [1]. An early solution in the process industry to reduce disturbance propagation in recycle systems was to install large surge tanks between interacting process units [2]. Large surge tanks are unlikely to be acceptable in amine scrubbing because of the added capital cost, along with oxidation, solid solubility, and safety issues associated with large amine hold-ups. Therefore, any storage tank in the plant will not be able to effectively dampen disturbances that propagate through the recycle streams.

In order to develop a plantwide control strategy for recycle systems with minimal inventory, the multiple time scale behavior that emerges as a result of material and energy recycling must be taken into consideration. There are two distinct time scales that exist in the amine scrubbing process dynamics: a fast time scale at the unit level associated with the large recycle flows and a slow time scale at the process level associated with the small feed and product flows. The time scales of the process variable will be identified using singular perturbation theory. Standard singularly perturbed model form is shown in Equations 1–2, where $\boldsymbol{\zeta}$ represents the slow variables, $\boldsymbol{\eta}$ the fast variables, and ε is some small parameter. Arranging the model of the amine scrubbing system in this form allows for the systematic identification of slow and fast variables. In the limit where $\varepsilon \rightarrow 0$, the left hand side of Equation 2 becomes zero and the fast variables are approximately at steady state [3].

$$\dot{\boldsymbol{\zeta}} = f(\boldsymbol{\zeta}, \boldsymbol{\eta}) \tag{1}$$

$$\varepsilon\dot{\boldsymbol{\eta}} = g(\boldsymbol{\zeta}, \boldsymbol{\eta}) \tag{2}$$

The objective of this work is to develop a reduced order model (ROM) with adjustable parameters that adequately represents the physical behavior of the true plant. The ROM is used for process simulation and time scale analysis. The ultimate goal of the ROM is its implementation in a model-based controller, which will be considered in future work.

Nomenclature

a	Wetted area [m^2/m^3]
C	Molar concentration [mol/m^3]
Cp	Specific heat capacity [kJ/mol·K]
D	Diameter [m]
d	Disturbance [-]
F	Molar flowrate [mol/s]
$\widehat{H}$	Specific enthalpy [kJ/mol]
h	Liquid hold-up in packing [m^3/m^3]
K	Overall mass transfer coefficient [mol/Pa·m^2·s]
K^p	Proportional gain constant [varies]
L	Length [m]
l	Level [m]
M	Molar amount [mol]
N	Transfer rate [amount/s]
Ns	Total number of column stages [-]
P	Pressure [Pa]
P^*	Equilibrium pressure of the liquid [Pa]
p_{CC}	Chilton-Colburn parameter [kJ/m^3·K]
Q_s	Steam heat duty [kW]
R	Gas constant [m^3·Pa/mol·K]
Rc	Recycle number [-]
T	Temperature [K]

UA	Overall heat transfer coefficient [kW/K]
u	Normalized manipulated input [-]
vf	Vapor fraction [mol/mol]
$\boldsymbol{x}$	State vector [varies]
x	Liquid apparent mole fraction [mol/mol]
y	Vapor mole fraction [mol/mol]
Greek	
ΔH	Specific heat of phase change [kJ/mol]
ε	Small perturbation parameter [-]
$\boldsymbol{\zeta}$	Vector of slow variables [varies]
$\boldsymbol{\eta}$	Vector of fast variables [varies]
ω	$\mathcal{O}(1)$ quantity [-]
Subscripts	
i	Component (CO_2, H_2O, PZ, N_2, or O_2)
k	Column stage number
H	Enthalpy
sp	Setpoint
Superscripts	
L	Liquid phase
s	Steady state
V	Vapor phase

2. Reduced Order Model Development and Validation

The model developed in this work is for the advanced amine scrubbing process using 8 molal (m) aqueous piperazine (PZ) described in Fig. 1 [4]. The ROM is nonlinear and based on first principles. Simplifications (discussed in the following paragraphs) have been made to the full first principles model, which results in a ROM that is appropriate for time scale analysis and use in a model-based controller. The ROM differential equations are given in Appendix A.

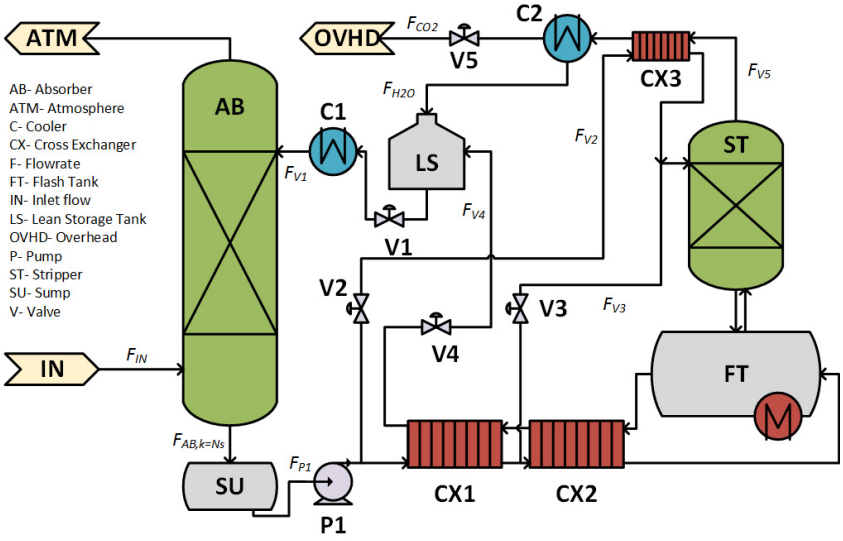

Fig. 1. Process flow diagram with advanced flash stripper configuration [4].

The absorber (AB) and stripper (ST), which contain structured packing, are modeled using constant rate-based mass and energy transfer coefficients that are multiplied by a driving force between the bulk liquid and bulk vapor (Equations 3–4).

$$N_i = K_i a \left(\frac{\pi D^2 L}{4}\right)(P_i - P_i^*),\ i = CO_2, H_2O \tag{3}$$

$$N_H = p_{CC}(K_{H2O}a)\left(\frac{\pi D^2 L}{4}\right)(RT^V)(T^V - T^L) \tag{4}$$

In the AB, the CO_2 mass transfer coefficient implicitly accounts for the rate enhancement due to chemical reaction. Equation 3 shows that bulk convection between the liquid and vapor is ignored. While ignoring bulk convection is a good assumption in the AB since the gas is mostly inert, it may cause deviation from the true

Table 1. ROM inputs, disturbances, and parameters.

Inputs and Disturbances	Thermo and Transport Parameters	Physical Parameters
$F_{V1}^L = 139{,}900\ mol/s$	$Cp^L = 0.11\ kJ/mol \cdot K$	$C^L = 35{,}700\ mol/m^3$
$F_{V2}^L = 0.15 \cdot F_{V1}^L$	$Cp^V = 0.03\ kJ/mol \cdot K$	$C_{AB}^V = 38\ mol/m^3$
$F_{V3}^L = 0.20 \cdot F_{V1}^L$	$\Delta H_{CO2} = 70\ kJ/mol$	$C_{ST}^V = 350\ mol/m^3$
$F_5^V = 2{,}920\ mol/s$	$\Delta H_{H2O} = 40\ kJ/mol$	$D_{AB} = 18\ m$
$Q_s = 385000\ kW$	$K_{AB,CO2}a = 4.83\ X\ 10^{-4}\ mol/Pa \cdot m^3 \cdot s$	$D_{SU} = 18\ m$
$F_{IN} = 18850\ mol/s$	$K_{AB,H2O}a = 1.16\ X\ 10^{-2}\ mol/Pa \cdot m^3 \cdot s$	$D_{FT} = 10.6\ m$
$T_{IN}^V = 313.15\ K$	$K_{ST,CO2}a = 9.66\ X\ 10^{-4}\ mol/Pa \cdot m^3 \cdot s$	$D_{ST} = 3\ m$
$y_{CO2,IN} = 0.147$	$K_{ST,H2O}a = 1.16\ X\ 10^{-2}\ mol/Pa \cdot m^3 \cdot s$	$D_{LS} = 10\ m$
$y_{N2,IN} = 0.752$	$p_{AB,CC} = 0.236\ kJ/m^3 \cdot K$	$h_{AB} = 0.05\ m^3/m^3$
$y_{O2,IN} = 0.027$	$p_{ST,CC} = 0.236\ kJ/m^3 \cdot K$	$h_{ST} = 0.05\ m^3/m^3$
$y_{H2O,IN} = 0.074$	$UA_{CX1} = 600{,}000\ kW/K$	$L_{AB} = 4.72\ m$
$l_{SU,sp}^L = 3\ m$	$UA_{CX2} = 300{,}000\ kW/K$	$L_{ST} = 2\ m$
$l_{FT,sp}^L = 3\ m$	$UA_{CX3} = 4{,}500\ kW/K$	$Ns_{AB} = 10$
		$Ns_{ST} = 4$
		$P_{AB} = 1\ bar$

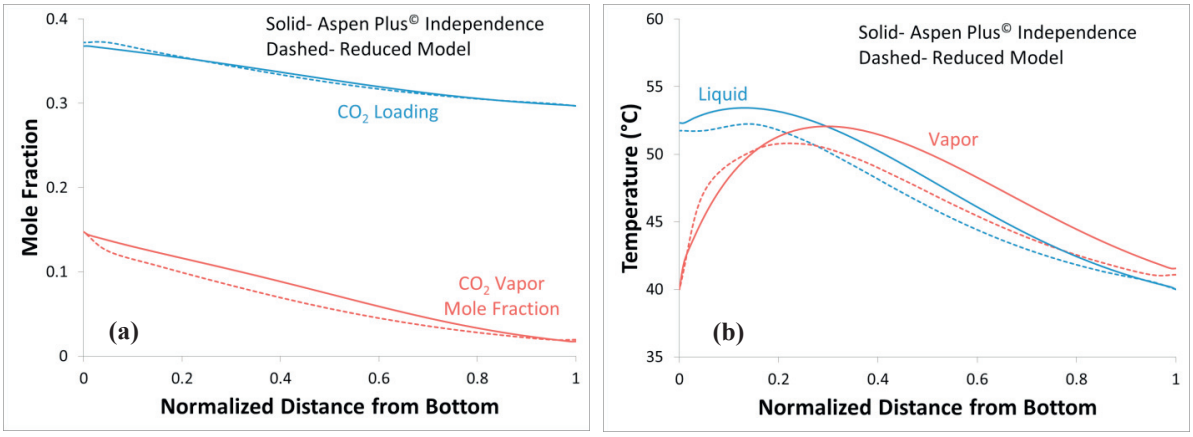

Fig. 2. Comparison of absorber (a) mole fraction and (b) temperature profiles for rigorous Aspen Plus® model [6] and ROM.

behavior of the plant in the ST. The heat transfer coefficient in Equation 4 is proportional to the H_2O mass transfer coefficient through the Chilton-Colburn analogy. The AB and ST packing are coarsely discretized into well-mixed segments for material and energy balances, which greatly reduces the number of model states compared to a finely discretized plug-flow regime. Liquid and vapor molar hold-ups at each segment are assumed to be constant, eliminating the total material balance in the columns.

Tanks, including the absorber sump (SU), flash tank (FT), and lean storage tank (LS) are treated as well-mixed equilibrium stages within the system. They each have material and energy balances on only the liquid hold-up. The main cross exchangers (CX1 and CX2) are assumed to exchange only sensible heat. This is likely a bad assumption for CX2 since flashing is known to occur in the rich solvent on the cold side of the exchanger. The ST and bypass exchanger (CX3) allow energy to be recovered from water vaporized in the FT by heating the bypass streams. It is assumed that heat is applied directly to the FT using steam from the power plant; the steam provides some sensible heat ($\Delta T \sim 5$ °C) and most of the latent heat requirement of the process. The trim cooler (C1) and overhead condenser (C2) are treated as perfect heat exchangers: the lean solvent fed to the absorber is always at 40 °C and all of the water vapor is condensed out of the overhead gas.

Everywhere in the system, PZ is assumed to be nonvolatile and N_2 and O_2 are treated as insoluble components. Thermophysical parameters such as molar density, heat capacity, and heat of absorption are assumed to be constant. Enthalpy and vapor-liquid equilibrium are calculated using the procedure described in Walters et al. [5]. Table 1 summarizes the parameters used in the ROM. The transfer coefficients in the AB are determined by minimizing the square error of the CO_2 mole fraction and temperature profiles between the ROM and a rigorous Aspen Plus® model [6] under the same conditions using 50 stages. In a true plant, uncertain parameters such as these could be found through a system identification. The AB column profiles of the Aspen Plus® and ROM are compared in Fig. 2. The ROM achieves an 86% CO_2 removal rate, while the Aspen Plus® model is designed for 90%. The largest absolute error in the temperature profile is 2.9 °C.

3. Time Scale Analysis

3.1. Material Recycle Number

A time scale analysis was performed on the ROM of the amine process based on the work of Baldea and Daoutidis [7]. Only the material balances have been considered here; energy recycle will be addressed in future work. Fig. 3 shows a rate-based AB where CO_2 is transferring into the solvent from the flue gas at all k segments. The recycle flowrate, F_{V1}, is much greater than the amount of CO_2 fluxing into the system. Furthermore, the flowrate of CO_2 in the lean solvent entering the AB is higher than the flowrate of CO_2 in the flue gas. A material recycle number, Rc, is defined in Equation 5 as the ratio of the large recycle flowrate to the small feed flowrate.

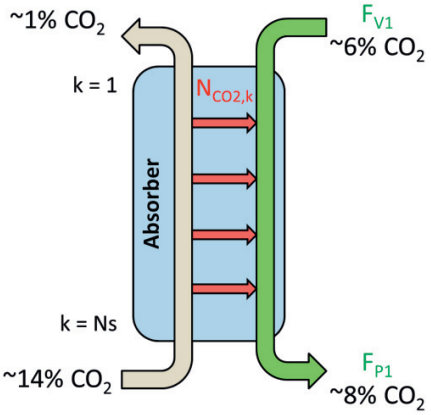

Fig. 3. CO_2 transfers from the flue gas to the liquid at each k segment of the column, but this flow is relatively small compared to the total liquid flow into the column.

$$Rc = \frac{1}{\varepsilon} = \frac{{F_{V1}}^s}{{N_{CO2,k=Ns}}^s} \tag{5}$$

The CO_2 flux is generally expected to be greatest at the bottom of the column, so the flux at the bottom segment is selected for the recycle number definition. An important implication of this selection is that the transfer rates at other segments of the column are of the same order of magnitude or less. The recycle number is substituted into the ROM described in Appendix A. For convenience, other dimensionless quantities have been defined in Table 2.

Table 2. Scaled quantities substituted into ROM.

Manipulated Inputs	Other Parameters
$u_1 = \frac{F_{V1}^L}{F_{V1}^{L\,s}}$	$\omega_2 = \frac{F_{V2}^{L\,s}}{F_{V1}^{L\,s}}$
$u_2 = \frac{F_{V2}^L}{F_{V2}^{L\,s}}$	$\omega_3 = \frac{F_{V3}^{L\,s}}{F_{V1}^{L\,s}}$
$u_3 = \frac{F_{V3}^L}{F_{V3}^{L\,s}}$	$\omega_4 = \frac{F_{V4}^{L\,s}}{F_{V1}^{L\,s}}$
$u_4 = \frac{F_{V4}^L}{F_{V4}^{L\,s}}$	$\omega_{AB,CO2,k} = \frac{{N_{AB,CO2,k}}^s}{{N_{AB,CO2,k=Ns}}^s}$
$u_5 = \frac{F_5^V}{F_5^{V\,s}}$	$d_{AB,i,k} = \frac{N_{AB,i,k}}{{N_{AB,i,k}}^s}$
$u_p = \frac{F_{P1}^L}{F_{P1}^{L\,s}}$	

3.2. Nonstandard Singularly Perturbed Model

After making the substitutions from Section 3.1, the model takes the form of Equation 6:

$$\dot{\boldsymbol{x}} = \boldsymbol{f}(\boldsymbol{x}) + \boldsymbol{G}_{sm}(\boldsymbol{x})\boldsymbol{u}_{sm} + \frac{1}{\varepsilon}\boldsymbol{G}_{lg}(\boldsymbol{x})\boldsymbol{u}_{lg} \tag{6}$$

where $\boldsymbol{x} \in \mathbb{R}^n$ is the state vector, $\boldsymbol{u}_{sm} \in \mathbb{R}^{m_{sm}}$ are the small inlet or outlet flows, $\boldsymbol{u}_{lg} \in \mathbb{R}^{m_{lg}}$ are the large internal flows, $\boldsymbol{f} \in \mathbb{R}^n$ is a vector of small flows which are a functions of the states, and $\boldsymbol{G}_{sm}$ and $\boldsymbol{G}_{lg}$ are matrices of appropriate dimensions. Equation 6 is referred to as nonstandard singularly perturbed form. Unlike the standard form given in Equations 1–2, the variables are not explicitly separated into slow and fast time scales in the nonstandard form. Equations 7–20 show the amine scrubbing ROM from Appendix A (excluding the energy balances and AB vapor material balances) in the form of Equation 6.

$$\dot{x}_{AB,CO2,k} = \frac{1}{M_{AB}^L}\Big[{N_{AB,CO2,k=Ns}}^s d_{AB,CO2,k}\omega_{AB,CO2,k} + x_{AB,CO2,k-1}\sum_{k=1}^{k-1} N_{AB,k} - x_{AB,CO2,k}\sum_{k=1}^{k} N_{AB,k} + \frac{1}{\varepsilon}u_1 {N_{AB,CO2,k=Ns}}^s\left(x_{AB,CO2,k-1} - x_{AB,CO2,k}\right)\Big] \tag{7}$$

$$\dot{x}_{AB,PZ,k} = \frac{1}{M_{AB}^L}\Big[x_{AB,PZ,k-1}\sum_{k=1}^{k-1} N_{AB,k} - x_{AB,PZ,k}\sum_{k=1}^{k} N_{AB,k} + \frac{1}{\varepsilon}u_1 {N_{AB,CO2,k=Ns}}^s\left(x_{AB,PZ,k-1} - x_{AB,PZ,k}\right)\Big] \tag{8}$$

$$\dot{x}_{ST,CO2,k} = \frac{1}{M_{ST}^L}\Big[N_{ST,CO2,k} + x_{ST,CO2,k-1}\sum_{k=1}^{k-1} N_{ST,k} - x_{ST,CO2,k}\sum_{k=1}^{k} N_{ST,k} + \frac{1}{\varepsilon}{N_{AB,CO2,k=1}}^s\left(x_{ST,CO2,k-1} - x_{ST,CO2,k}\right)(u_2\omega_2 + u_3\omega_3)\Big] \tag{9}$$

$$\dot{x}_{ST,PZ,k} = \frac{1}{M_{ST}^{L}}\left[x_{ST,PZ,k-1}\sum_{k=1}^{k-1}N_{ST,k} - x_{ST,PZ,k}\sum_{k=1}^{k}N_{ST,k} + \frac{1}{\varepsilon}N_{AB,CO2,k=1}{}^{s}\left(x_{ST,PZ,k-1} - x_{ST,PZ,k}\right)(u_2\omega_2 + u_3\omega_3)\right] \quad (10)$$

$$\dot{y}_{ST,CO2,k} = \frac{1}{M_{ST,k}^{V}}\left[\left(y_{ST,CO2,k+1} - y_{ST,CO2,k}\right)\left(u_5 F_{V5}^{V\ s} + \sum_{k=1}^{k-1}N_{ST,k}\right) + y_{ST,CO2,k+1}N_{ST,k} - N_{ST,CO2,k}\right] \quad (11)$$

$$\dot{l}_{SU}^{L} = \frac{4}{\pi {D_{SU}}^2 C^L}\left[\sum_{k=1}^{N_s}N_{AB,k} + \frac{1}{\varepsilon}N_{AB,CO2,k=Ns}{}^{s}\left(u_1 - \omega_p u_P\right)\right] \quad (12)$$

$$\dot{x}_{SU,CO2} = \frac{4}{\pi {D_{SU}}^2 C^L l_{SU}^{L}}\left[\sum_{k=1}^{N_s}N_{AB,k}\left(x_{AB,CO2,k=N_s} - x_{SU,CO2}\right) + \frac{1}{\varepsilon}N_{AB,CO2,k=Ns}{}^{s}u_1\left(x_{AB,CO2,k=N_s} - x_{SU,CO2}\right)\right] \quad (13)$$

$$\dot{x}_{SU,PZ} = \frac{4}{\pi {D_{SU}}^2 C^L l_{SU}^{L}}\left[\sum_{k=1}^{N_s}N_{AB,k}\left(x_{AB,PZ,k=N_s} - x_{SU,PZ}\right) + \frac{1}{\varepsilon}N_{AB,CO2,k=Ns}{}^{s}u_1\left(x_{AB,PZ,k=N_s} - x_{SU,PZ}\right)\right] \quad (14)$$

$$\dot{l}_{FT}^{L} = \frac{4}{\pi {D_{FT}}^2 C^L}\left[-u_5 F_{V5}^{V\ s} + \frac{1}{\varepsilon}N_{AB,CO2,k=1}{}^{s}(\omega_p u_p - \omega_4 u_4)\right] \quad (15)$$

$$\dot{x}_{FT,CO2} = \frac{4}{\pi {D_{FT}}^2 C^L l_{FT}^{L}}\left[\left(x_{ST,CO2,k=Ns} - y_{FT,CO2}\right)\sum_{k=1}^{N_s}N_{ST,k} + \left(x_{FT,CO2} - y_{FT,CO2}\right)u_5 F_{V5}^{V\ s} + \frac{1}{\varepsilon}N_{AB,CO2,k=1}{}^{s}\left(\left(x_{SU,CO2} - x_{FT,CO2}\right)u_p\omega_p + \left(x_{ST,CO2,k=Ns} - x_{SU,CO2}\right)(u_2\omega_2 + u_3\omega_3)\right)\right] \quad (16)$$

$$\dot{x}_{FT,PZ} = \frac{4}{\pi {D_{FT}}^2 C^L l_{FT}^{L}}\left[x_{ST,PZ,k=Ns}\sum_{k=1}^{N_s}N_{ST,k} + x_{FT,PZ}u_5 F_{V5}^{V\ s} + \frac{1}{\varepsilon}N_{AB,CO2,k=1}{}^{s}\left(\left(x_{SU,PZ} - x_{FT,PZ}\right)u_p\omega_p + \left(x_{ST,PZ,k=Ns} - x_{SU,PZ}\right)(u_2\omega_2 + u_3\omega_3)\right)\right] \quad (17)$$

$$\dot{l}_{LS}^{L} = \frac{4}{\pi {D_{LS}}^2 C^L}\left[F_{H2O}^{L} + \frac{1}{\varepsilon}N_{AB,CO2,k=1}{}^{s}(\omega_4 u_4 - u_1)\right] \quad (18)$$

$$\dot{x}_{LS,CO2} = \frac{4}{\pi {D_{LS}}^2 C^L l_{LS}^{L}}\left[-x_{LS,CO2}F_{H2O}^{L} + \frac{1}{\varepsilon}N_{AB,CO2,k=1}{}^{s}\omega_4 u_4\left(x_{FT,CO2} - x_{LS,CO2}\right)\right] \quad (19)$$

$$\dot{x}_{LS,PZ} = \frac{4}{\pi {D_{LS}}^2 C^L l_{LS}^{L}}\left[-x_{LS,PZ}F_{H2O}^{L} + \frac{1}{\varepsilon}N_{AB,CO2,k=1}{}^{s}\omega_4 u_4\left(x_{FT,PZ} - x_{LS,PZ}\right)\right] \quad (20)$$

In the context of Equation 6, $\boldsymbol{u}_{sm} = u_5$ and $\boldsymbol{u}_{lg} = \left[u_1\ u_2\ u_3\ u_4\ u_p\right]^T$. The only states that are exclusively slow ($\boldsymbol{G}_{lg} = \boldsymbol{0}$) are the ST vapor mole fractions in Equation 11. All other state variables have both slow and fast components. Fig. 3 demonstrates the pseudo-open loop response of the process to a 10% step reduction in flue gas rate after one hour of steady state operation. The total material balances (Equations 12, 15, and 18) render the system open loop unstable, so perfect level control is assumed in the SU, FT, and LS during the simulation. It is also assumed that the water makeup rate is perfectly controlled so the LS concentration is always 8 m PZ. The AB liquid mole fractions (Fig. 3a) have an initial fast response at the unit level as the amount of CO_2 entering the system is decreased. The fast response is followed by a slow transient period as the system approaches a new steady state. The ST vapor mole fractions (Fig. 3b) are only affected by the small outlet flowrate and therefore only demonstrate a slow response to the step change.

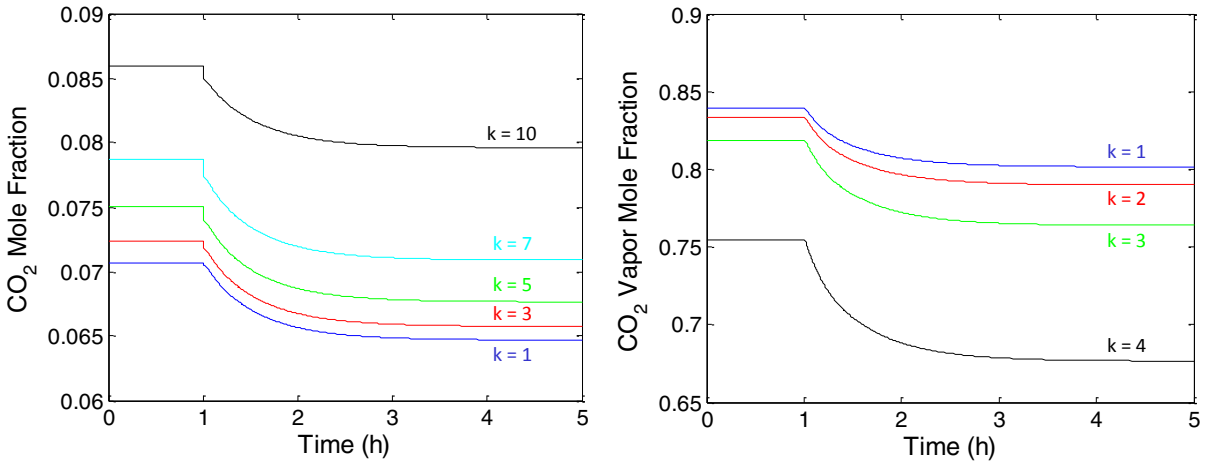

Fig. 3. Pseudo-open loop response to a 10% decrease in flue gas flow after one hour for (a) the AB liquid mole fractions and (b) the ST vapor mole fractions at segment k of the column.

3.3. Standard Singularly Perturbed Model

In model-based control of a process with time scale multiplicity, the process model needs to be explicitly separated into fast and slow variables [8]. The SU, FT, and LS unit inventories must be stabilized based on the fast time scale, so it is assumed that there is a linear state feedback controller for the tank levels that manipulates the tank effluent flow. Since the energy balance has not yet been taken into consideration, it is also assumed that there is a state feedback law for the exiting cross exchange temperatures ($T_{CX1,h}$ and $T_{CX3,h}$) that manipulates the bypass flowrates. The feedback control laws are given in Equations 21–25, which show that the large flowrates are now a function of the states.

$$u_1 = 1 - K_1^p\left(l_{LS} - l_{LS,sp}\right) \tag{21}$$

$$u_2 = 1 - K_2^p\left(T_{CX3,h}^L - T_{CX3,h,sp}^L\right) \tag{22}$$

$$u_3 = 1 - K_3^p\left(T_{CX3,h}^L - T_{CX3,h,sp}^L\right) \tag{23}$$

$$u_4 = 1 - K_4^p\left(l_{FT} - l_{FT,sp}\right) \tag{24}$$

$$u_p = 1 - K_p^p\left(l_{SU} - l_{SU,sp}\right) \tag{25}$$

It is assumed that the matrix $\boldsymbol{G}_{lg}(\boldsymbol{x})$ can be decomposed according to Equation 26:

$$\boldsymbol{G}_{lg}(\boldsymbol{x}) = \boldsymbol{B}(\boldsymbol{x})\widetilde{\boldsymbol{G}}_{lg}(\boldsymbol{x}) \tag{26}$$

where $\boldsymbol{B} \in \mathbb{R}^{n\times(n-3-Ns_{ST})}$ is a full column rank matrix and $\widetilde{\boldsymbol{G}}_{lg} \in \mathbb{R}^{(n-3-Ns_{ST})\times m_{lg}}$ is a matrix with linearly independent rows [9]. The variable transformation $\mathbf{T}(\mathbf{x})$ in Equation 27 is applied to explicitly separate the ROM into slow and fast states:

$$\begin{bmatrix}\boldsymbol{\zeta}\\ \boldsymbol{\eta}\end{bmatrix} = \boldsymbol{T}(\boldsymbol{x}) = \begin{bmatrix} M_{total} \\ M_{total,CO2} \\ M_{total,PZ} \\ y_{ST,CO2,k=1} \\ \vdots \\ y_{ST,CO2,k} \\ \vdots \\ y_{ST,CO2,k=Ns} \\ \widetilde{\boldsymbol{G}}_{lg}(\boldsymbol{x})\boldsymbol{u}_{lg}(\boldsymbol{x}) \end{bmatrix} \tag{27}$$

where $\boldsymbol{\zeta} \in \mathbb{R}^{3+Ns_{ST}}$ are the slow states, $\boldsymbol{\eta} \in \mathbb{R}^{n-3-Ns_{ST}}$ are the fast states, and the subscript total denotes the total system molar hold-up. This transformation allows the ROM to be arranged in the form of Equations 1–2, and shows that the total molar hold-ups also evolve on the slow time scale in addition to the stripper vapor mole fractions. Fig. 4 demonstrates the step response of the total system CO_2 hold-up has only a slow component. The steady state liquid residence times in the AB, SU, FT, ST, and LS are 0.3, 3.2, 1.1, 0.02, and 0.9 minutes, respectively, while Fig. 4 shows that the time constant of total CO_2 inventory is ~32 minutes. The total plant inventory time constant is an order of magnitude higher than the individual unit operation residence times because of the material recycle occurring in the process.

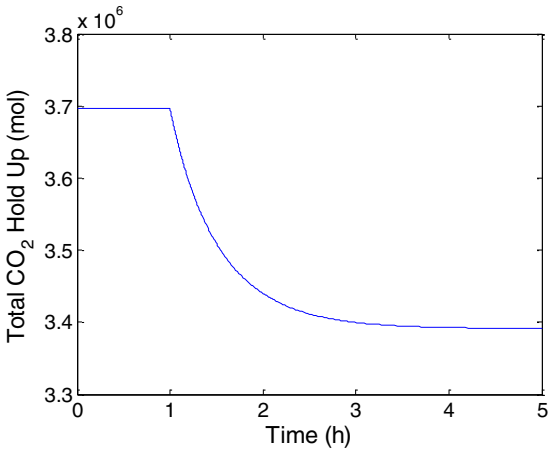

Fig. 4. Pseudo-open loop response to a 10% decrease in flue gas flow after one hour for the total CO_2 inventory.

4. Proposed Control Structure

The overall control objective of the amine scrubbing process is to maintain a desired CO_2 removal rate while minimizing energy use. Additionally, the total material holdup must be stabilized. Based on the singularly perturbed model form, both of these control objectives are related to the slow time scale. In the previous section, state feedback control laws were proposed for the large internal solvent flows in order to stabilize the system on the fast time scale. The only remaining manipulated variable for the slow time scale objectives is the stripper overhead flowrate (F_{V5}^{V}). F_{V5}^{V} is closely tied to the flowrate of CO_2 out of the process, so it should be used to control the removal rate. Since there are no more remaining manipulated variables, the total inventory setpoint can be manipulated by changing the level setpoint on the LS. This structure cascades the fast time scale level control objective with the slow time scale total inventory objective.

Previous work has proposed controlling the removal rate with the large internal recycle flow [10]. However, this strategy will likely lead to an ill-conditioned controller based on the time scale analysis since the slow time scale has not been addressed. Oscillations in stripper pressure were observed by Ziaii when the removal rate was controlled

using the solvent flowrate [11]. The control structure proposed in this work is summarized in Table 3. A state space realization of the slow time scale for use in a model-based controller can be achieved by taking the limit $\varepsilon \rightarrow 0$ (corresponding to infinite recycle) in Equations 1–2. This control structure will be evaluated in future work.

Table 3. Scaled quantities substituted into ROM

Time Scale	Output Variable	Input Variable	Proposed Controller
Fast	Sump Level	Sump Effluent Flowrate (F_{P1})	Proportional
	Flash Tank Level	Recycle Flowrate (F_{V4})	Proportional
	Lean Storage Tank Level	Solvent Flowrate (F_{V1})	Proportional
Slow	Total Material Hold-up	Lean Storage Tank Level Setpoint ($l_{LS,sp}$)	Cascaded, Model-Based
	CO_2 Removal Rate	Stripper Overhead Flowrate (F_{V5})	Model-Based

5. Conclusions

Two time scales exist in the amine scrubbing process dynamics as a result of material recycling. The ROM developed for the time scale analysis and model-based control was compared to a rigorous Aspen Plus® Rate-Sep model. The temperature profile of the ROM is within 2.9 °C of Aspen Plus® model and CO_2 removal rate is within 4%. The time scale decomposition shows that the stripper vapor mole fractions and total system inventories evolve on the slow time scale only. Therefore the CO_2 removal rate and total material hold-up should be controlled using the small stripper overhead flow and fast time scale setpoints. Controlling CO_2 removal with the large solvent recycle flowrate will likely lead to oscillations in process variables.

Acknowledgments

The authors acknowledge the financial support of the Texas Carbon Management Program.

The authors declare the following competing financial interest(s): One author of this publication consults for Southern Company and for Neumann Systems Group on the development of amine scrubbing technology. The terms of this arrangement have been reviewed and approved by the University of Texas at Austin in accordance with its policy on objectivity in research. The authors have financial interests in intellectual property owned by the University of Texas that includes ideas reported in this paper.

Appendix A. Reduced Order Model Material and Energy Balances

The liquid side balances for the absorber are given in Equations 28–29, with the boundary conditions at k = 0 of $F^L_{AB,k=0} = F^L_{V1}$, $x_{AB,i,k=0} = x_{LS,i}$, and $\widehat{H}^L_{AB,k=0} = \widehat{H}^L_{LS}$. The vapor side balances are shown in Equations 30–31, with the boundary conditions at k = Ns + 1 of $F^V_{AB,k=Ns+1} = F^V_{IN}$, $y_{AB,i,k=Ns+1} = y_{IN,i}$, and $\widehat{H}^V_{AB,k=Ns+1} = \widehat{H}^V_{IN}$.

$$\dot{M}^L_{AB,i,k} = x_{AB,i,k-1}F^L_{AB,k-1} - x_{AB,i,k}F^L_{AB,k} + N_{AB,i,k},\ i = CO_2, PZ \tag{28}$$

$$\dot{T}^L_{AB,k} = \frac{1}{Cp^L M^L_{AB,k}}\left[\widehat{H}^L_{AB,k-1}F^L_{AB,k-1} - \widehat{H}^L_{AB,k}F^L_{AB,k} + N_{AB,H,k}\right] + \frac{1}{Cp^L}\left[(\Delta H_{CO2} - \Delta H_{H2O})\dot{x}_{AB,CO2,k} - \Delta H_{H2O}\dot{x}_{AB,PZ,k}\right] \tag{29}$$

$$\dot{M}^V_{AB,i,k} = y_{AB,i,k+1}F^V_{AB,k+1} - y_{AB,i,k}F^V_{AB,k} - N_{AB,CO2,k},\ i = CO_2, N_2, O_2 \tag{30}$$

$$\dot{T}^V_{AB,k} = \frac{1}{Cp^V M^V_{AB,k}}\left[\hat{H}^V_{AB,k+1}F^V_{AB,k+1} - \hat{H}^V_{AB,k}F^V_{AB,k} - N_{AB,H,k}\right] \quad (31)$$

The liquid side balances for the stripper are given in Equations 32–33, with the boundary conditions at k = 0 of $F^L_{ST,k=0} = F^L_{V2} + F^L_{V3}$, $x_{ST,i,k=0} = x_{SU,i}$, and $\hat{H}^L_{AB,k=0} = (\hat{H}^L_{CX3,c}F^L_{V2} + \hat{H}^L_{CX1,c}F^L_{V3})/(F^L_{V2} + F^L_{V3})$. The vapor side balances are shown in Equations 34–35, with the boundary conditions at k = 0 of $F^V_{AB,k=0} = F^V_{V5}$ and at k = Ns + 1 of $y_{ST,i,k=Ns+1} = y_{FT,i}$ and $\hat{H}^V_{ST,k=Ns+1} = \hat{H}^V_{FT}$.

$$\dot{M}^L_{ST,i,k} = x_{ST,i,k-1}F^L_{ST,k-1} - x_{ST,i,k}F^L_{ST,k} + N_{ST,i,k},\ i = CO_2, PZ \quad (32)$$

$$\dot{H}^L_{ST,k} = \hat{H}^L_{ST,k-1}F^L_{ST,k-1} - \hat{H}^L_{ST,k}F^L_{ST,k} + N_{ST,H,k} \quad (33)$$

$$\dot{M}^V_{ST,CO2,k} = y_{ST,CO2,k+1}F^V_{ST,k+1} - y_{ST,CO2,k}F^V_{ST,k} - N_{ST,CO2,k} \quad (34)$$

$$\dot{H}^V_{ST,k} = \hat{H}^V_{ST,k+1}F^V_{ST,k+1} - \hat{H}^V_{ST,k}F^V_{ST,k} - N_{ST,H,k} \quad (35)$$

The material and energy balances for the sump, flash tank, and lean storage tank are all treated as well mixed liquid stages in Equations 36–44.

$$\dot{M}^L_{SU} = F^L_{AB,k=N_s} - F^L_{P1} \quad (36)$$

$$\dot{M}^L_{SU,i} = x_{AB,i,k=N_s}F^L_{AB,k=N_s} - x_{SU,i}F^L_{P1},\ i = CO_2, PZ \quad (37)$$

$$\dot{T}^L_{SU} = \frac{1}{Cp^L M^L_{SU}}\left[\hat{H}^L_{AB,k=N_s}F^L_{AB,k=N_s} - \hat{H}^L_{SU}F^L_{P1}\right] + \frac{1}{Cp^L}\left[(\Delta H_{CO2} - \Delta H_{H2O})\dot{x}_{SU,CO2} - \Delta H_{H2O}\dot{x}_{SU,PZ}\right] \quad (38)$$

$$\dot{M}^L_{FT} = F^L_{P1} - F^L_{V4} - F^V_{V5} \quad (39)$$

$$\dot{M}^L_{FT,i} = x_{SU,i}(F^L_{P1} - F^L_{V2} - F^L_{V3}) + x_{ST,i,k=Ns}F^L_{ST,k=Ns} - x_{FT,i}F^L_{V4} - y_{FT,i}\left(F^V_{ST,k=Ns} + N_{ST,k=N_s}\right),\ i = CO_2, PZ \quad (40)$$

$$\dot{T}^L_{FT} = \frac{1}{Cp^L M^L_{FT}}\left[\hat{H}^L_{CX2,c}(F^L_{P1} - F^L_{V2} - F^L_{V3}) + \hat{H}^L_{ST,k=Ns}F^L_{ST,k=Ns} - \hat{H}^L_{FT}F^L_{V4} - \hat{H}^V_{FT}\left(F^V_{ST,k=Ns} + N_{ST,k=N_s}\right) + Q_s\right] + \frac{1}{Cp^L}\left[(\Delta H_{CO2} - \Delta H_{H2O})\dot{x}_{FT,CO2} - \Delta H_{H2O}\dot{x}_{FT,PZ}\right] \quad (41)$$

$$\dot{M}^L_{LS} = F^L_{V4} + F^L_{H2O} - F^L_{V1} \quad (42)$$

$$\dot{M}^L_{LS,i} = x_{FT,i}F^L_{V4} - x_{LS,i}F^L_{V1},\ i = CO_2, PZ \quad (43)$$

$$\dot{T}^L_{LS} = \frac{1}{Cp^L M^L_{LS}}\left[\hat{H}^L_{FT}F^L_{V4} + \hat{H}^L_{H2O}F^L_{H2O} - \hat{H}^L_{LS}F^L_{V1}\right] + \frac{1}{Cp^L}\left[(\Delta H_{CO2} - \Delta H_{H2O})\dot{x}_{LS,CO2} - \Delta H_{H2O}\dot{x}_{LS,PZ}\right] \quad (44)$$

The energy balance for the cross heat exchangers is given in Equations 45–50, where the energy flux, N_H, is calculated by multiplying the overall heat transfer coefficient by a log mean driving force.

$$\dot{T}^L_{CX1,c} = \frac{1}{Cp^L M^L_{CX1,c}}\left[\left(T^L_{SU} - T^L_{CX1,c}\right)(F^L_{P1} - F^L_{V2}) + N_{CX1,H}\right] + \frac{1}{Cp^L}\left[(\Delta H_{CO2} - \Delta H_{H2O})\dot{x}_{SU,CO2} - \Delta H_{H2O}\dot{x}_{SU,PZ}\right] \quad (45)$$

$$\dot{T}^L_{CX1,h} = \frac{1}{Cp^L M^L_{CX1,h}}\left[\left(T^L_{CX2,h} - T^L_{CX1,h}\right)F^L_{V4} - N_{CX1,H}\right] + \frac{1}{Cp^L}\left[(\Delta H_{CO2} - \Delta H_{H2O})\dot{x}_{FT,CO2} - \Delta H_{H2O}\dot{x}_{FT,PZ}\right] \quad (46)$$

$$\dot{T}^L_{CX2,c} = \frac{1}{Cp^L M^L_{CX2,c}}\left[\left(T^L_{CX1,c} - T^L_{CX2,c}\right)\left(F^L_{P1} - F^L_{V2} - F^L_{V3}\right) + N_{CX2,H}\right] + \frac{1}{Cp^L}\left[\left(\Delta H_{CO2} - \Delta H_{H2O}\right)\dot{x}_{SU,CO2} - \Delta H_{H2O}\dot{x}_{SU,PZ}\right] \quad (47)$$

$$\dot{T}^L_{CX2,h} = \frac{1}{Cp^L M^L_{CX2,h}}\left[\left(T^L_{FT} - T^L_{CX2,h}\right)F^L_{V4} - N_{CX2,H}\right] + \frac{1}{Cp^L}\left[\left(\Delta H_{CO2} - \Delta H_{H2O}\right)\dot{x}_{FT,CO2} - \Delta H_{H2O}\dot{x}_{FT,PZ}\right] \quad (48)$$

$$\dot{T}^L_{CX3,c} = \frac{1}{Cp^L M^L_{CX3,c}}\left[\left(T^L_{SU} - T^L_{CX3,c}\right)F^L_{V2} + N_{CX3,H}\right] + \frac{1}{Cp^L}\left[\left(\Delta H_{CO2} - \Delta H_{H2O}\right)\dot{x}_{SU,CO2} - \Delta H_{H2O}\dot{x}_{SU,PZ}\right] \quad (49)$$

$$\dot{T}^L_{CX3,h} = \frac{1}{Cp^L M^L_{CX3,h}}\left[\widehat{H}^V_{ST,k=1}F^V_{V5} - \widehat{H}^L_{CX3,h}(1 - vf_{CO2})F^T_{V5} - \widehat{H}^V_{CX3,h}vf_{CO2}F^T_{V5} - N_{CX3,H}\right] \quad (50)$$

References

[1] Luyben WL. Dynamics and Control of Recycle Systems. 1. Simple Open-Loop and Closed-Loop Systems. Ind Eng Chem Res 1993;32:466-75.

[2] Seborg DE, Edgar TF, Mellichamp DA, Doyle FJ. Process Dynamics and Control, 3rd Ed. Hoboken, NJ: John Wiley & Sons; 2011.

[3] Kokotović P, Khalil HK, O'Rielly J. Singular Perturbation Methods in Control: Analysis and Design. London: Academic Press; 1986.

[4] Lin Y-J, Madan T, Rochelle GT. Regeneration with Rich Bypass of Aqueous Piperazine and Monoethanolamine for CO_2 Capture. Ind Eng Chem Res 2014;53:4067-74.

[5] Walters MS, Dunia RH, Edgar TF, Rochelle GT. Two-Stage Flash for CO_2 Regeneration: Dynamic Modeling and Pilot Plant Validation. Energy Procedia 2013;37:2133-44.

[6] Frailie PT. Modeling of Carbon Dioxide Absorption/Stripping by Aqueous Methyldiethanolamine/Piperazine. The University of Texas at Austin. Ph.D. Dissertation. 2014.

[7] Baldea M, Daoutidis P. Dynamics and Nonlinear Control of Integrated Process Systems. New York: Cambridge University Press; 2012.

[8] Chen X, Heidarinejad M, Liu J, Christofides PD. Composite Fast-Slow MPC Design for Nonlinear Singularly Perturbed Systems. AIChE J 2012;58:1802-11.

[9] Baldea M, Daoutidis P. A General Analysis and Control Framework for Process Systems with Inventory Recycling. Int J Robust Nonlin 2013;In Press.

[10] Panahi M, Karimi M, Skogestad S, Hillestad M, Svendsen HF. Self-Optimizing and Control Structure Design for a CO_2 Capturing Plant. 2nd Ann Gas Proc Symp, Qatar. 2010.

[11] Ziaii, SF. Dynamic Modeling, Optimization, and Control of Monoethanolamine Scrubbing for CO_2 Capture. The University of Texas at Austin. Ph.D. Dissertation. 2012.